J|A|C|S
ARTICLES
Published on Web 11/17/2006

Resolution of Chiral Phosphate, Phosphonate, and Phosphinate Esters by an Enantioselective Enzyme Library

Charity Nowlan,[§] Yingchun Li,[§] Johannes C. Hermann,[‡] Timothy Evans,[§] Joseph Carpenter,[§] Eman Ghanem,[§] Brian K. Shoichet,*[,‡] and Frank M. Raushel*[,§]

Contribution from the Department of Chemistry, P.O. Box 30012, Texas A&M University, College Station, Texas 77842-3012, and Department of Pharmaceutical Chemistry, University of California, San Francisco, MC 2550, 1700 4th Street, San Francisco, California 94158-2230

Received August 11, 2006; E-mail: shoichet@cgl.ucsf.edu; raushel@tamu.edu

Abstract: An array of 16 enantiomeric pairs of chiral phosphate, phosphonate, and phosphinate esters was used to establish the breadth of the stereoselective discrimination inherent within the bacterial phosphotriesterase and 15 mutant enzymes. For each substrate, the leaving group was 4-hydroxyacetophenone while the other two groups attached to the phosphorus core consisted of an asymmetric mixture of methyl, methoxy, ethyl, ethoxy, isopropoxy, phenyl, phenoxy, cyclohexyl, and cyclohexoxy substituents. For the wild-type enzyme, the relative rates of hydrolysis for the two enantiomers ranged from 3 to 5.4×10^5. Various combinations of site-specific mutations within the active site were used to create modified enzymes with alterations in their enantioselective properties. For the single-site mutant enzyme, G60A, the stereoselectivity is enhanced relative to that of the wild-type enzyme by 1−3 orders of magnitude. Additional mutants were obtained where the stereoselectivity is inverted relative to the wild-type enzyme for 13 of the 16 pairs of enantiomers tested for this investigation. The most dramatic example was obtained for the hydrolysis of 4-acetylphenyl methyl phenyl phosphate. The G60A mutant preferentially hydrolyzes the S_P-enantiomer by a factor of 3.7×10^5. The I106G/F132G/H257Y mutant preferentially hydrolyzes the R_P-enantiomer by a factor of 9.7×10^2. This represents an enantioselective discrimination of 3.6×10^8 between these two mutants, with a total of only four amino acid changes. The rate differential between the two enantiomers for any given mutant enzyme is postulated to be governed by the degree of nonproductive binding within the enzyme active site and stabilization of the transition state. This hypothesis is supported by computational docking of the high-energy, pentavalent form of the substrates to modeled structures of the mutant enzyme; the energies of the docked transition-state analogues qualitatively capture the enantiomeric preferences of the various mutants for the different substrates. These results demonstrate that the catalytic properties of the wild-type phosphotriesterase can be exploited for the kinetic resolution of a wide range of phosphate, phosphonate, and phosphinate esters and that the active site of this enzyme is remarkably amenable to structural perturbations via amino acid substitution.

Introduction

Enzymes have become powerful tools in the synthesis of value-added chemicals from cheaper and more readily available starting materials.[1] For example, the catalytic activity of xylose isomerase is currently being exploited for the preparation of 3 million tons of high-fructose corn syrup per year via the isomerization of D-glucose.[2] D-Hydantoinases are employed in the kinetic resolution of racemic mixtures of D-phenylglycine and D-*p*-hydroxy-phenylglycine for the semisynthesis of penicillins with annual production runs of several thousand tons.[3] Relative to chemical catalysts, the most significant advantages possessed by enzymes are the extraordinary rate enhancements and the high degree of selectivity for chiral centers. However, many wild-type enzymes exhibit a rather narrow substrate specificity that can limit the range of useful and practical applications. Nevertheless, recent advances in the construction and assay of mutant protein libraries have demonstrated that in vitro evolution of existing enzyme templates can result in the enhancement and expansion of catalytic function for a desired chemical transformation.[4]

The bacterial phosphotriesterase (PTE) catalyzes the hydrolysis of activated organophosphate triesters as shown in Scheme 1 for the detoxification of the insecticide paraoxon, with kinetic constants $k_{cat} \approx 10^4$ s^{-1} and $k_{cat}/K_m \approx 10^8$ M^{-1} s^{-1}.[5] The substrate specificity is rather broad, and the wild-type enzyme is able to distinguish between enantiomers that are chiral at the phosphorus center.[6,7] The substantial catalytic activity of phos-

[§] Texas A&M University.
[‡] University of California, San Francisco.

(1) Liese, A. In *Enzyme Catalysis in Organic Synthesis*; Drauz, K., Waldmann, H., Eds.; Wiley-VCH: Weinheim, Germany, 2002; Vol. III, pp 1419−1459.
(2) Esaki, N.; Kurihara, T.; Soda, K. In *Enzyme Catalysis in Organic Synthesis*; Drauz, K., Waldmann, H., Eds.; Wiley-VCH: Weinheim, Germany, 2002; Vol. III, pp 1281−1332.
(3) Syldatk, C.; Muller, R.; Siemann, M.; Wagner, F. In *Biocatalytic Production of Amino Acids and Derivatives*; Rozzell, D., Wagner, F., Eds.; Hanser Publishers: Munchen, Germany, 1992; pp 75−128.
(4) Minshull, J.; Stemmer, W. *Curr. Opin. Biotechnol.* **1999**, *35*, 48−51.
(5) Aubert, S. D.; Li, Y.; Raushel, F. M. *Biochemistry* **2004**, *43*, 5707−5715.

10.1021/ja0658618 CCC: $33.50

Scheme 1

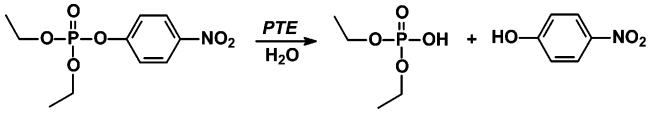

photriesterase is ideally suited for a variety of chemical transformations. For example, PTE is one of the predominant enzymes under current consideration as the primary catalytic component for the detection and degradation of chemical threat agents such as sarin, soman, and VX.[8] The detoxification of agricultural and household organophosphate insecticides is a logical extension of this technology, and commercial insecticides may be enzymatically resolved by PTE into separate enantiomers that are differentially toxic to specific insect targets.[9] The enantioselective properties of PTE may be applicable to the resolution of chiral phosphorus containing pro-drugs and the chemo-enzymatic syntheses of chiral phosphine ligands for transition metal catalysts.[10,11] Unlike chiral carbon centers, there is no reservoir of naturally occurring chiral phosphorus centers that can be chemically transformed to the target of choice.

If the catalytic potential of PTE is to be exploited for the kinetic resolution of chiral phosphorus centers, then the substrate specificity and stereoselectivity must be expanded and enhanced. Prior work with lipases and hydantoinases suggests that manipulation of the amino acid sequence can result in the production of enzyme variants with altered catalytic properties.[12,13] For example, Reetz and colleagues have elegantly shown that directed evolution of a lipase from *Pseudomonas aeruginosa* can be utilized to enhance the stereoselectivity for the hydrolysis of *p*-nitrophenyl 2-methyl decanoate from an initial value of 1.1 to >51 via a combination of error-prone mutagenesis, gene shuffling, and saturation mutagenesis.[14] Only six amino acid changes from the wild-type sequence were required to achieve this result. Even more impressive, the same strategy was used to identify mutant proteins with the opposite stereoselectivity. A mutant with 11 amino acid changes was isolated that favored the other enantiomer by a factor of 30.[15] Many, but not all, of the amino acid substitutions were located away from the active site, and a molecular explanation for the changes in catalytic properties is not generally obvious.[16]

In this paper, we have probed the stereoselective properties of the wild-type PTE and selected mutant enzymes. The breadth of the substrate specificity has been addressed with a series of racemic mixtures of fully esterified phosphate, phosphonate, and phosphinate derivatives. The structural diversity for members of this library of substrates is shown in Chart 1. We

Chart 1

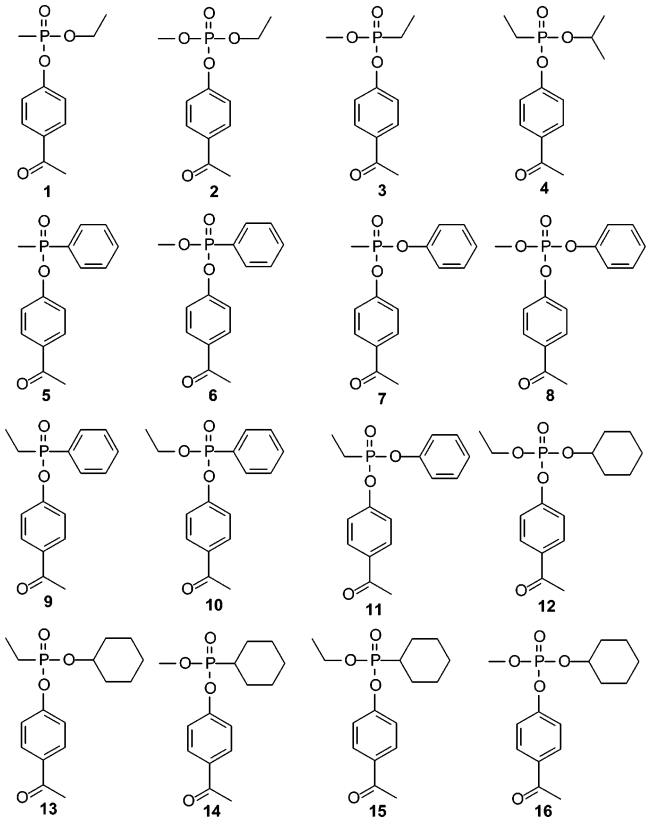

demonstrate that the inherent enantioselectivity of the wild-type PTE can be greater than 10^5 and can be further enhanced up to 3 orders of magnitude by a single amino acid change to the active site. We also establish that a relatively small number of amino acid changes within the active site can invert the stereoselectivity of the wild-type enzyme and favor the opposite enantiomer by up to 3 orders of magnitude. In the most dramatic example, the differences in stereoselectivity for each enantiomer can be as high as 100 million for two mutants that differ by only four amino acids.

Materials and Methods

Materials. The bacterial phosphotriesterase and the site-directed mutants were prepared and purified to homogeneity as previously described.[6,7,17] Methylphenylphosphinic chloride was obtained from Acros Organics. The other chemicals involved in the synthesis of the substrates for phosphotriesterase were obtained from Aldrich. ^{1}H and ^{31}P NMR spectra in $CDCl_3$ were obtained on Varian Unity INOVA spectrometers. The ^{31}P NMR spectra were obtained with phosphoric acid (85%) as the external reference. Exact mass measurements were obtained on a PE Sciex APJ Qstar Pulsar by the Laboratory for Biological Mass Spectrometry at Texas A&M University.

Synthesis of Racemic Substrates. The phosphate, phosphonate, and phosphinate esters synthesized for this investigation are depicted in Chart 1. Compounds **1**−**4**, **6**−**8**, and **10**−**16** were prepared according to the general procedure described below. Triethylamine (1 equiv) was added dropwise into a stirred mixture of an alkyl phosphonic dichloride or alkyl dichlorophosphate (10−20 mmol) and the corresponding alcohol or phenol (1 equiv) in ethyl ether or dichloromethane (~100 mL) at 0 °C. After the reaction mixture was stirred for 3−8 h, *p*-hydroxyacetophenone (1 equiv) was added, along with another portion

(6) Chen-Goodspeed, M.; Sogorb, M. A.; Wu, F.; Hong, S.-B.; Raushel, F. M. *Biochemistry* **2001**, *40*, 1325−1331.
(7) Chen-Goodspeed, M.; Sogorb, M. A.; Wu, F.; Raushel, F. M. *Biochemistry* **2002**, *40*, 1332−1339.
(8) Raushel, F. M. *Curr. Opin. Microbiol.* **2002**, *5*, 288−295.
(9) Miyazaki, A.; Najamura, T.; Kawaradani, M.; Marumo, S. *J. Agric. Food Chem.* **1988**, *36*, 835−837.
(10) Reddy, K. R.; Boyer, S. H.; Erion, M. D. *Tetrahedron Lett.* **2005**, *46*, 4321−4324.
(11) Pietrusiewicz, K. M.; Zablocka, M. *Chem. Rev.* **1994**, *94*, 1375−1411.
(12) May, O.; Nyuyen, P. T.; Arnold, F. H. *Nat. Biotechnol.* **2000**, *18*, 317−320.
(13) Reetz, M. T.; Zonta, A.; Schimossek, L.; Liebeton, K.; Jaeger, L.-E. *Angew. Chem.* **1997**, *109*, 2961−2963.
(14) Reetz, M. T.; Wilensek, S.; Zha, D.; Jaeger, L.-E. *Angew. Chem.* **2001**, *113*, 3701−3703.
(15) Zha, D.; Wilensek, S.; Hermes, J.; Jaeger, K.-E.; Reetz, M. T. *Chem. Commun*. **2001**, 2664−2665.
(16) Bocola, M.; Otte, N.; Jaeger, K.-E.; Reetz, M. T.; Thiel, W. *Chem. Biol. Chem.* **2004**, *5*, 214−223.
(17) Hill, C. M.; Li, W.-S.; Thoden, J. B.; Holden, H. M.; Raushel, F. M. *J. Am. Chem. Soc.* **2003**, *125*, 8990−8991.

of triethylamine (1 equiv). The reaction mixture was stirred at room temperature for another 24−48 h, and then the triethylammonium chloride was removed by filtration. The reaction mixture was condensed to dryness under reduced pressure. The residue was applied to a column of silica gel and eluted with a mixture of hexanes and ethyl acetate. A general workup gave the desired compounds in yields ranging from 20 to 85%.

4-Acetylphenyl ethyl methylphosphonate (**1**) was prepared from methyl phosphonic dichloride and ethanol. ^{1}H NMR (ppm): 7.98 (2H, d, J = 9.0 Hz), 7.30 (2H, d, J = 9.0 Hz), 4.08−4.30 (2H, m), 2.60 (3 H, s), 1.66 (3H, d, J = 17.8 Hz), 1.35 (3H, t, J = 7.2 Hz). ^{31}P NMR (ppm): 33.0. Mass spectrometry (ESI positive ion mode for M + H): calculated, 243.08; found, 243.08.

4-Acetylphenyl ethyl methyl phosphate (**2**) was prepared from methyl dichlorophosphate and ethanol. ^{1}H NMR (ppm): 7.98 (2H, d, J = 9.0 Hz), 7.30 (2H, d, J = 9.0 Hz), 4.22 (2H, m), 3.84 (3H, d, J = 11.8 Hz), 2.60 (3H, s), 1.98 (3H, t, J = 7.2 Hz). ^{31}P NMR (ppm): −5.04. Mass spectrometry (ESI positive ion mode for M + H): calculated, 259.07; found, 259.08.

4-Acetylphenyl methyl ethylphosphonate (**3**) was prepared from ethyl phosphonic dichloride and methanol. ^{1}H NMR (ppm): 7.98 (2H, d, J = 9.0 Hz), 7.30 (2H, d, J = 9.0 Hz), 3.84 (3H, d, J = 11.8 Hz), 2.60 (3H, s), 1.84−2.00 (2H, m), 1.24 (3H, dt, J = 19.7 Hz, J = 7.3 Hz). ^{31}P NMR (ppm): 37.0. Mass spectrometry (ESI positive ion mode for M + H): calculated, 243.08; found, 243.08.

4-Acetylphenyl isopropyl ethylphosphonate (**4**) was prepared from ethylphosphonic dichloride and isopropyl alcohol. ^{1}H NMR (ppm): 7.98 (2H, d, J = 9.0 Hz), 7.30 (2H, d, J = 9.0 Hz), 4.80 (1H, m), 2.60 (3H, s), 1.82−1.98 (2H, m), 1.98−2.18 (9H, m). ^{31}P NMR (ppm): 34.3. Mass spectrometry (ESI positive ion mode for M + H): calculated, 271.11; found, 271.11.

4-Acetylphenyl methyl(phenyl)phosphinate (**5**) was prepared upon mixing a solution of methyl(phenyl)phosphinic chloride (20 mmol) in ethyl ether (100 mL) with a saturated solution of 4-hydroxyacetophenone (20 mmol) in ethyl ether and stirred at 0 °C. Triethylamine (20 mmol) was added dropwise, and the reaction mixture was stirred at room temperature for 42 h. After removal of the solvent under reduced pressure, the residue was applied to a column of silica gel and eluted with a mixture of hexanes and ethyl acetate (1:1, v/v). ^{1}H NMR (ppm): 7.78−7.88 (4H, m), 7.42−7.60 (3H, m), 7.20 (2H, d, J = 9.0 Hz), 2.49 (3H, s), 1.90 (3H, d, J = 17.8 Hz). ^{31}P NMR (ppm): 50.6. Mass spectrometry (ESI positive ion mode for M + H): calculated, 275.08; found, 275.08.

4-Acetylphenyl methyl phenylphosphonate (**6**) was prepared from phenyphosphonic dichloride and methanol. ^{1}H NMR (ppm): 7.82−7.87 (4H, m), 7.58−7.62 (1H, m), 7.44−7.54 (2H, m), 7.27 (2H, d, J = 8 Hz), 3.90 (3H, d, J = 11 Hz), 2.48 (3H, s). ^{31}P NMR (ppm): 20.3. Mass spectrometry (ESI positive ion mode for M + H): calculated, 291.08; found, 291.08.

4-Acetylphenyl phenyl methylphosphonate (**7**) was prepared from methylphosphonic dichloride and phenol. ^{1}H NMR (ppm): 7.80 (2H, d, J = 9.0 Hz), 7.20−7.40 (7H, m), 2.60 (3H, s), 1.86 (3H, d, J = 17.8 Hz). ^{31}P NMR (ppm): 29.8. Mass spectrometry (ESI positive ion mode for M + H): calculated, 291.08; found 291.09.

4-Acetylphenyl methyl phenyl phosphate (**8**) was prepared from methyl dichlorophosphate and phenol. ^{1}H NMR (ppm): 7.98 (2H, d, J = 9.0 Hz), 7.15−7.5 (7H, m), 3.98 (3H, d, J = 11.8 Hz), 2.58 (3H, s). ^{31}P NMR (ppm): −10.7. Mass spectrometry (ESI positive ion mode for M + H): calculated, 307.07; found, 307.08.

4-Acetylphenyl ethyl(phenyl)phosphinate (**9**) was prepared by mixing diethyl phenylphosphonite (28 mmol) and ethyl iodide (3.2 mmol) in a sealed tube and stirred at 95 °C for 48 h. Volatiles were removed under reduced pressure. The reaction mixture was dissolved in ethyl ether (200 mL) and washed with sodium sulfate (10% aqueous solution) until the reaction solution was colorless. Removal of the ether gave ethyl ethyl(phenyl)phosphinate (4.2 g) with a yield of 78%. Ethyl ethyl(phenyl)phosphinate (2.5 mmol) was mixed with oxalyl chloride (3.8 mmol) and stirred at room temperature under dry conditions for 40 min. After removal of the volatile components under reduced pressure, the residue was dissolved in ethyl ether (15 mL), and then 4-hydroxyacetophenone (2.4 mmol) and triethylamine (2.4 mmol) were added. After the reaction mixture was stirred at room temperature for 24 h, it was filtered and condensed to dryness under reduced pressure. The residue was applied to a column of silica gel and eluted with a mixture of hexanes and ethyl acetate (1:2, v/v). ^{1}H NMR (ppm): 7.82−7.88 (4 H, m), 7.56−7.60 (1H, m), 7.24−7.26 (2H, d, J = 9.0 Hz), 2.58 (3H, s), 2.04−2.24 (2H, m), 1.22 (3H, dt, J = 19.7 Hz, J = 7.3 Hz). ^{31}P NMR (ppm): 53.9. Mass spectrometry (ESI positive ion mode for M + H): calculated, 289.10; found, 289.11.

4-Acetylphenyl ethyl phenylphosphonate (**10**) was prepared from phenylphosphonic dichloride and ethanol. ^{1}H NMR (ppm): 7.80−7.85 (4H, m), 7.52−7.60 (1H, m), 7.44−7.48 (2H, m), 7.22−7.30 (2H, d, J = 9.0 Hz), 4.20−4.30 (2H, m), 2.58 (3H, s), 1.36−1.40 (3H, t, J = 7.2 Hz). ^{31}P NMR (ppm): 18.5. Mass spectrometry (ESI positive ion mode for M + H): calculated, 305.09; found, 305.10.

4-Acetylphenyl phenyl ethylphosphonate (**11**) was prepared from ethylphosphonic dichloride and phenol. ^{1}H NMR (ppm): 7.94 (2H, d, J = 9.0 Hz), 7.37−7.15 (7H, m), 2.58 (3H, s), 2.19−2.09 (2H, m), 1.41−1.34 (3H, dt, J_{H-P} = 21.8 Hz, J_{H-H} = 7.8 Hz). ^{31}P NMR (ppm): 28.4. Mass spectrometry (ESI positive ion mode for M + H): calculated, 305.09; found, 305.10.

4-Acetylphenyl cyclohexyl ethyl phosphate (**12**) was prepared from ethyl dichlorophosphate and cyclohexanol. ^{1}H NMR (ppm): 7.98 (2H, d, J = 9.0 Hz), 7.30 (2H, d, J = 9.0 Hz), 4.50 (1H, m), 4.20 (2H, m), 2.58 (3H, s), 1.20−2.02 (13H, m). ^{31}P NMR (ppm): −7.10. Mass spectrometry (ESI positive ion mode for M + H): calculated, 327.14; found, 327.14.

4-Acetylphenyl cyclohexyl ethylphosphonate (**13**) was prepared from ethylphosphonic dichloride and cyclohenxanol. ^{1}H NMR (ppm): 7.98 (2H, d, J = 9.0 Hz), 7.30 (2H, d, J = 9.0 Hz), 4.55 (1H, m), 2.60 (3H, s), 1.20−2.02 (16H, m). ^{31}P NMR (ppm): 34.0. Mass spectrometry (ESI positive ion mode for M + H): calculated, 311.14; found, 311.14.

4-Acetylphenyl methyl cyclohexylphosphonate (**14**) was prepared from cyclohexylphosphonic dichloride and methanol. ^{1}H NMR (ppm): 7.98 (2H, d, J = 9.0 Hz), 7.30 (2H, d, J = 9.0 Hz), 3.80 (3H, d, J = 11.8 Hz), 2.58 (3H, s), 1.20−2.10 (11H, m). ^{31}P NMR (ppm): 35.0. Mass spectrometry (ESI positive ion mode for M + H): calculated, 297.12; found, 297.13.

4-Acetylphenyl ethyl cyclohexylphosphonate (**15**) was prepared from cyclohexylphosphonic dichloride and ethanol. ^{1}H NMR (ppm): 7.98 (2H, d, J = 9.0 Hz), 7.30 (2H, d, J = 9.0 Hz), 4.04−4.24 (2H, m), 2.58 (3H, s), 1.20−2.10 (14 H, m). ^{31}P NMR (ppm): 33.7. Mass spectrometry: (ESI positive mode for M + H): calculated, 311.14; found, 311.14.

4-Acetylphenyl cyclohexyl methyl phosphate (**16**) was prepared from methyl dichlorophosphate and cyclohexanol. ^{1}H NMR (ppm): 7.98 (2H, d, J = 9.0 Hz), 7.29 (2H, d, J = 9.0 Hz), 4.3 (1H, m), 3.85 (3H, d, J = 11.8 Hz), 2.60 (3H, s), 1.2−2.0 (10H, m). ^{31}P NMR (ppm): −5.88. Mass spectrometry (ESI positive ion mode for M + H): calculated, 313.12; found, 313.12.

Assay of Catalytic Properties. The time courses for the hydrolysis of the racemic mixtures of substrates were monitored at 294 nm using a SpectraMax360 UV−vis spectrophotometer. The extinction coefficient used for 4-hydroxyacetophenone was 7.71×10^3 M^{-1} cm^{-1}. Enzyme was added to the substrate in a final volume of 3.0 mL, containing 50 mM CHES buffer, pH 9.0. The initial concentration of the racemic substrates varied from 50 to 100 μM. The change in absorbance was recorded, and the data were fit to either eq 1 or eq 2,

$$A_t = A_o + A_1(1 - e^{-k_1 t}) \quad (1)$$

$$A_t = A_o + A_1(1 - e^{-k_1 t}) + A_2(1 - e^{-k_2 t}) \quad (2)$$

where A_t is the absorbance at any time t, A_o is the initial absorbance, A_1 and A_2 are net absorbance changes for the individual phases of the reaction, and k_1 and k_2 are the first-order rate constants for each phase. The Michaelis constants for a representative selection of substrates were measured and found to be greater than 300 μM.

Docking Calculations. Full details of the docking methods are given in the accompanying paper.[33] Briefly, structures for a number of the PTE mutant enzymes were generated. These mutant enzymes differed from the wild type by only a few specific residues, and these residues were positioned such that their side chains projected into ligand open regions of the active site. The substitutions either reduce or extend the mutated side chain, but no major backbone movements are expected. Consistent with this view, the actual X-ray structure of the H254G/H257W/L303T mutant differs from that of the wild-type PTE by an RMSD of only 0.27 Å.[17−19] Therefore, we were conservative in our model building, holding the structure of the overall enzyme constant, and only modified the position of the substituting side chains themselves. Beginning with the wild-type structure (PDB code 1HZY[18]), substituted residues were fit into the structure by keeping the coordinates of as many common atoms as possible. A dockable molecular database was calculated that contained the pentavalent, bipyramidal high-energy intermediate forms of 11 of the 16 experimentally tested enantiomeric pairs. This flexibase was generated in analogy to the ZINC database;[20] the primary innovation was the creation of pentavalent structures which were obtained by modifications on the SMILES level followed by multiconformer structure calculations using Corina and Omega.[21,22] These structures resemble the compounds in the state after nucleophilic attack of the catalytic hydroxide on the phosphorus and should represent a state which the enzyme will preferentially recognize, enabling finer distinctions.[23] This database was docked into the active sites of PTE and its mutants using DOCK3.5.54 and scored on the basis of van der Waals and electrostatic complementarity, corrected for ligand desolvation energies. For each pair of enantiomers, the difference of their docking energy scores was calculated and used as a proxy for the binding affinity.

Results and Discussion

Chiral Substrate Library. The breadth of the substrate specificity exhibited by the bacterial phosphotriesterase was established by measuring the relative kinetic constants for a broad series of phosphate, phosphonate, and phosphinate esters. The leaving group for the entire series of compounds was 4-hydroxyacetophenone because the enzymatic formation of this compound in solution at pH 9 can be easily monitored at 294 nm without interference from the protein or the initial substrate ester. The remaining two groups, attached directly to the phosphorus center, included methyl, methoxy, ethyl, ethoxy, isopropoxy, cyclohexyl, cyclohexoxy, phenyl, and phenoxy substituents. These side chains provided a reasonable array of steric bulk and the inclusion of hydrophobic and hydrophilic atoms for direct molecular interactions within the active site of PTE. The nine substituents were mixed to generate a small but diverse chemical library of racemic mixtures that included two phosphinates, four phosphates, and ten phosphonates. The structures of the compounds used in this investigation are presented in Chart 1.

Measurement of Stereoselectivity for Wild-Type PTE. The relative rate of hydrolysis for each of the two enantiomers within the 16 racemic mixtures was obtained by monitoring the full time course (based on the end-point analysis for hydrolysis with KOH) for each of the two isomers immediately after the addition of an appropriate amount of enzyme. The initial concentration of the ester substrate was established by hydrolysis with an appropriate amount of hydroxide. For example, in Figure 1A is shown the time course for the chemical hydrolysis of compound **6** with 67 mM NaOH. The hydrolysis reaction follows first-order kinetics, and a fit of the data to eq 1 yields a rate constant of 0.25 min^{-1}. The time courses for the enzymatic hydrolysis of **6** with 2.0 (gray line) and 200 nM (red line) wild-type PTE are presented in Figure 1B. The time course for the lower amount of enzyme clearly indicates that one of the two enantiomers is hydrolyzed significantly faster than the other, since only one-half of the total substrate is hydrolyzed in 10 min. At substrate concentrations lower than the Michaelis constant, the time courses follow pseudo-first-order kinetics, and the associated rate constants are directly proportional to the amount of enzyme added.[24] The rate constant from a fit of the data to eq 1 is 0.47 min^{-1}. Dividing the first-order rate constant by the concentration of enzyme provides $k_{cat}/K_m \approx 3.9 \times 10^6\ M^{-1}\ s^{-1}$. At the higher level of enzyme, the fast phase is essentially complete during the mixing time prior to data acquisition. A fit of the data to eq 1 gives a rate constant of 0.24 min^{-1} and a value of k_{cat}/K_m for the slow enantiomer of $\sim 2.0 \times 10^4\ M^{-1}\ s^{-1}$ after correction for the amount of enzyme added. The ratio of rates for the hydrolysis of the fast and slow enantiomers of **6** is 200. Similar experiments were conducted for the other 15 pairs of enantiomers, and the results are presented in Table 1. In certain cases (such as with compounds **1**−**4**), the times courses for both enantiomers could be obtained with a single concentration of enzyme. In these instances, the data were fit to eq 2 to provide the rate constants for both phases. For compounds **1**−**16**, the degree of discrimination between the two enantiomers ranges from ~3 for compounds **1** and **2** to 5.4×10^5 for compound **12**.

Stereoselectivity for the Mutant G60A. The enantioselectivities for the G60A mutant of PTE were determined for the library of phosphate, phosphonate, and phosphinate esters in the same manner as described for the wild-type enzyme. Presented in Figure 1C are the time courses for the hydrolysis of compound **6** with 0.50 nM (gray line) and 20 μM (red line) G60A. The mutant enzyme clearly hydrolyzes one enantiomer at a significantly faster rate than the other enantiomer. A fit of the time course for the lower level of enzyme to eq 1 provides a first-order rate constant of 0.91 min^{-1}. Correcting for the amount of enzyme gives a value $k_{cat}/K_m \approx 3.0 \times 10^7\ M^{-1}\ s^{-1}$ for the faster of the two enantiomers. Similarly, the rate constant from a fit of the time course for the more concentrated enzyme gives a first-order rate constant of 0.43 min^{-1} and a value of $k_{cat}/K_m \approx 360\ M^{-1}\ s^{-1}$. The mutant G60A prefers one isomer by a factor of 8.3×10^4. Similar experiments were conducted for the rest of the racemic mixtures, and in every case (except for compound **3**) the G60A mutant is more enantioselective than

(18) Benning, M. M.; Shim, H.; Raushel, F. M.; Holden, H. M. *Biochemistry* **2001**, *40*, 2712−2722.
(19) Benning, M. M.; Hong, S.-B.; Raushel, F. M.; Holden, H. M. *J. Biol. Chem.* **2000**, *275*, 30556−30560.
(20) Irwin, J.J.; Shoichet, B. K. *J. Chem. Inf. Model.* **2005**, *45*, 177−182.
(21) Sadowski, J.; Schwab, C. H.; Gasteiger, J. 3D Structure Generation and Conformational Searching. In *Computational Medicinal Chemistry and Drug Discovery*; Bultinck, P., De Winter, H., Langenaeker, W., Tollenaere, J. P., Eds.; Dekker Inc.: New York, 2003; pp 151−212.
(22) Bostrom, J.; Greenwood, J. R.; Gottfries, J. *J. Mol. Graphics Modell.* **2003**, *21*, 449−462.
(23) Pauling, L. *Chem. Eng. News* **1946**, *24*, 1375−1377.
(24) Cleland, W. W. In *The Enzymes*; Boyer, P. D., Ed.; Academic Press: New York, 1970; Vol. II, pp 1−65.

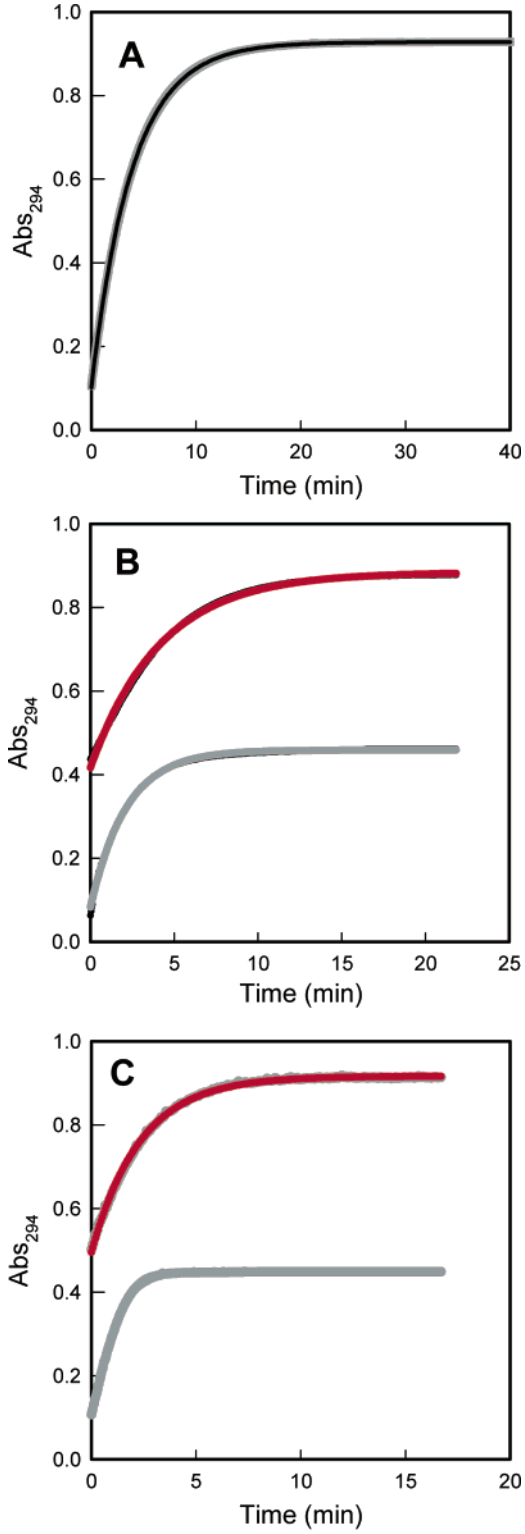

Figure 1. (A) Time course for the hydrolysis of compound **6** with 67 mM KOH. (B) Time course for the enzymatic hydrolysis of compound **6** with 2.0 nM PTE (gray line) and 200 nM wild-type PTE (red line) at pH 9.0 in 50 mM CHES buffer, 30 °C. (C) Time course for the enzymatic hydrolysis of compound **6** with 0.5 nM (gray line) and 20 μM (red line) concentrations of the G60A mutant of PTE. Additional details are provided in the text.

is the wild-type enzyme. The most extreme case is for compound **16**, where the stereoselectivity is greater than 6 million to one. The enantioselective ratios for the hydrolysis of racemic mixtures of chiral phosphorus esters by the mutant G60A are provided in Table 1.

Relaxation of Enantioselectivity. A selected set of mutant enzymes that were obtained by alteration of those residues that interact directly with the substrate within the active site of PTE were tested with the small library of phosphorus containing esters to ascertain the degree of change in the enantioselective properties. Shown in Figure 2A are the time courses for the hydrolysis of compound **8** at two different levels of enzyme. At a concentration of wild-type PTE of 1.9 nM, one-half of the racemic mixture is hydrolyzed with a first-order rate constant of 0.61 min^{-1} (gray line). This corresponds to a value of $k_{cat}/K_m \approx 5.4 \times 10^6$ M^{-1} s^{-1}. At a concentration of wild-type PTE of 190 nM, the fast enantiomer is hydrolyzed during the mixing of enzyme with substrate and the slow enantiomer is hydrolyzed with a first-order rate constant of 0.50 min^{-1}, obtained from a fit of the data to eq 1 (red line in Figure 2A). This corresponds to a value of $k_{cat}/K_m \approx 4.4 \times 10^4$ M^{-1} s^{-1}. The stereoselective preference of the wild-type enzyme for compound **8** is thus 120. Similar experiments with the G60A mutant established a stereoselective preference of 3.9×10^5. When compound **8** is hydrolyzed by the mutant H257Y (180 nM), both enantiomers are hydrolyzed at nearly identical rates, as shown for the time course presented in Figure 2B. A fit to eq 2 for the double exponential gives rate constants of 0.27 and 0.16 min^{-1}. The corresponding values of k_{cat}/K_m are $\sim 2.5 \times 10^4$ and $\sim 1.5 \times 10^4$ M^{-1} s^{-1}, respectively, with a rather low enantioselective preference of ~ 2.

Reversal of Stereoselectivity. For the mutant I106G/F132G/H257Y, the addition of high and low concentrations of enzyme demonstrated that the enzyme has a stereoselective preference of 970 for one enantiomer over the other (data not shown). In order to determine whether the stereoselectivity of this mutant is the same as or opposite to that possessed by the wild-type and G60A enzymes, a low level of the triple mutant (34 nM) was added to compound **8** to selectively hydrolyze the more rapidly hydrolyzed enantiomer. The time course for this experiment is presented in Figure 2C (gray line). After the hydrolysis of the more rapidly hydrolyzed enantiomer was complete, a low level of the G60A mutant was added to the reaction mixture to determine if the enantiomer preferred by the triple mutant was the same as that preferred by the G60A mutant. The time course for the addition of the G60A mutant (2.6 nM) is presented in Figure 2C (red line). Clearly, the G60A and I106G/F132G/H257Y mutants preferentially hydrolyze different enantiomers of compound **8**. Similar experiments were utilized to establish the stereoselective preferences for 15 mutants in addition to the wild-type PTE, and the results are presented in Table 1. Not every mutant was tested with every enantiomeric pair of substrates.

Absolute Stereochemistry. For the wild-type and G60A mutant enzymes, it has been demonstrated that the enantiomer hydrolyzed preferentially can be determined on the basis of the relative size and orientation of the substituents attached to the central phosphorus core.[25−29] For the target substrates constructed for this investigation, the pairs of enantiomers are

(25) Hong, S.-B.; Raushel, F. M. *Biochemistry* **1999**, *38*, 1159−1165.
(26) Wu, F.; Li, W.-S.; Chen-Goodspeed, M.; Sogorb, M.; Raushel, F. M. *J. Am. Chem. Soc.* **2000**, *122*, 10206−10207.
(27) Li, W.; Li, Y.; Hill, C. M.; Lum, K. T.; Raushel, F. M. *J. Am. Chem. Soc.* **2002**, *124*, 3498−3499.
(28) Li, Y.; Aubert, S. D.; Raushel, F. M. *J. Am. Chem. Soc.* **2003**, *125*, 7526−7527.
(29) Li, Y.; Aubert, S. D.; Maes, E. G.; Raushel, F. M. *J. Am. Chem. Soc.* **2004**, *126*, 8888−8889.

Table 1. Enantioselectivity for Wild-Type PTE and Selected Mutants

Compound	*WT*	G60A	I106G	F132G	H257Y	S308G	I106G F132G	H257Y L303T	I106G H257Y	H254G H257R	I106G F132G H257Y	I106A H257Y S308A	I106A F132A H257W	H254R H257A L303T	H254R H257S L303T	I106T F132A H254G H257W
1 (R_P)[a]	3	20						**(43)**[b]			**(12)**	**(15)**	**(110)**		**(83)**	**(90)**
2 (S_P)	3	33						**6**			[4][c]	[5]	**(20)**	[5]		**(6)**
3	12	6						1		12	1	1			20	73
4 (R_P)	9	380						**(17)**		[3]	**(18)**	**(23)**	**(120)**		**(12)**	**(51)**
5 (S_P)	2900	$1.7x10^5$	$1.1x10^4$	2400	18	2000	2400	**(34)**	8		8	[4]	**(8)**	[3]		**(7)**
6 (S_P)	210	$8.3x10^4$	1200	9000	11	2300	$1.5x10^4$	**(18)**	14	54	21	3		2		32
7 (R_P)	89	$7.3x10^4$	8		**(12)**	110	1	**(10)**			**(730)**					**(790)**
8 (S_P)	120	$3.7x10^5$	12	100	**[2]**	470	[3]	[3]	**(560)**		**(970)**					**(22)**
9 (S_P)	5000	$8.6x10^5$		100				[3]			[4]	1	[3]	1		1
10 (S_P)	1100	$9.3x10^5$						1			610		110	67	9	380
11 (R_P)	130	$4.1x10^4$	3	7	1		**(29)**	7			**(940)**					**(930)**
12 (S_P)	$5.4x10^5$	$2.8x10^6$					7	340	[3]	>100	**(14)**	8	5		>100	8
13 (R_P)	$4.4x10^4$	$5.9x10^5$		>100	5900		[5]	16			**(58)**	[5]	**(16)**	24		**(39)**
14 (S_P)	83	$1.7x10^4$						**(1800)**			1					11
15 (S_P)	1600	$1.9x10^4$						**(10)**			19				25	180
16 (S_P)	$7.8x10^4$	$6.3x10^6$						1	**(24)**		**(64)**					6

[a] The absolute stereochemistries of the enantiomers preferred by the WT and G60A mutant forms of PTE are indicated, except for **3**. [b] When the stereoselective preference of the mutant is inverted from the preference of the wild-type and G60A forms of PTE, the stereoselectivity ratio is in red and in parentheses. [c] When the stereoselectivity ratio of the mutant is less than a factor of 5, the enantioselectivity, relative to the wild-type and mutant G60A, could not easily be determined, and the numbers are placed within brackets.

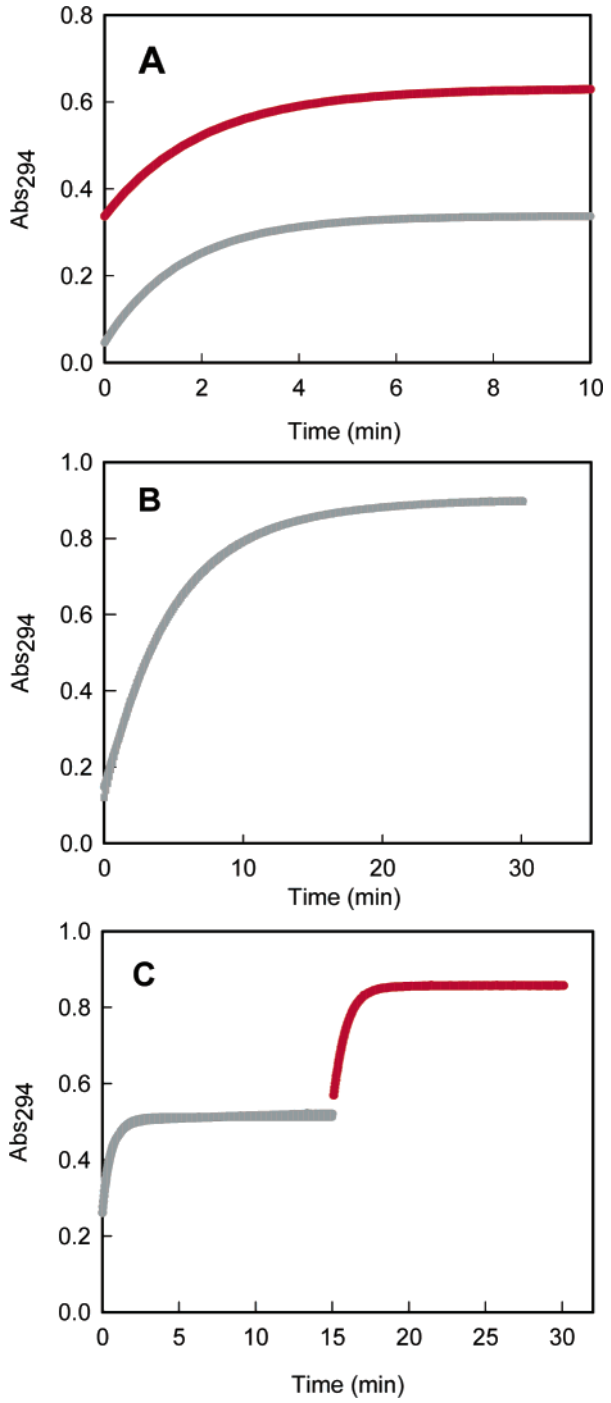

Figure 2. (A) Time course for the hydrolysis of compound **8** with 1.9 nM (gray line) and 190 nM (red line) wild-type PTE at pH 8.0 in 50 mM HEPES buffer, 25 °C. (B) Time course for the hydrolysis of compound **8** with a 180 nM concentration of the H257Y mutant of PTE. (C) Time course for the hydrolysis of the preferred enantiomer of compound **8** with a 34 nM concentration of the I106G/F132G/H257Y mutant of PTE (gray line). After hydrolysis of the preferred enantiomer of compound **8** (15 min), a 2.6 nM concentration of the mutant G60A was added to hydrolyze the remaining material (red line). Additional details are provided in the text.

presented as shown in Chart 1. The more rapidly hydrolyzed enantiomer is the one where the substituent oriented to the right in a Fischer projection is physically larger than the substituent orientated to the left. This enables the preferred enantiomer to be identified for the wild-type and G60A mutant forms of PTE, except for compound **3**, where the relative size of the two substituents is essentially the same. The stereochemically preferred enantiomer for the wild-type and G60A mutant is listed in Table 1. The notation changes for the phosphate, phosphonate, and phosphinate esters because of the nomenclature rules. A Brønsted analysis of the effect of the pK_a of the leaving group on k_{cat} and k_{cat}/K_m has shown that the β_{lg} for the wild-type enzyme is −1.8, and thus the substituted phenol (pK_a = 8.0) is always hydrolyzed rather than phenol (pK_a = 10) or any of the alcohols.[30]

Substrate Specificity. In this study, we have utilized nine different substituents attached to a central phosphorus core to create a small library of phosphate, phosphonate, and phosphinate esters. The wild-type and G60A variants are able to efficiently hydrolyze these compounds, and thus PTE has the ability to recognize and hydrolyze a rather diverse set of substrates while simultaneously exhibiting a rather pronounced stereoselectivity. For the wild-type enzyme, a clear stereochemical preference can be demonstrated for 14 of the 16 compounds tested. A significant distinction could not be demonstrated for methyl versus ethoxy or methoxy versus ethoxy as they exist in compounds **1** and **2**, where the stereochemical preference between the two enantiomers is less than 5. However, the stereoselectivity for the G60A mutant is significantly more pronounced than for the wild-type enzyme, and a clear distinction can be identified for all pairs of substituents, except for methoxy versus ethyl (compound **3**). For the wild-type enzyme, when the difference in size between the two substituents is one or two carbon/oxygen atoms, the inherent stereoselectivity is less than an order of magnitude (see compounds **1**−**4**). When a phenolic group is paired with a small alkyl or alkoxy substituent (see compounds **7**, **8**, and **11**), the preferred enantiomer is hydrolyzed about 2 orders of magnitude faster than the slower enantiomer. When the larger substituent is either phenyl or cyclohexyl, the degree of discrimination between the two enantiomers is greater than a factor of 10^3. In every case, except for compound **3**, the stereoselectivity is further enhanced by the mutant G60A. This increase in the stereoselectivity varies from 1 to 3 orders of magnitude by a single amino acid substitution within the active site of PTE. With compounds **12** and **16**, the rate differential between the two enantiomers is greater than a million-fold!

Inversion and Relaxation of Stereoselectivity. Single amino acid changes within the active site of PTE can relax the inherent stereoselectivity of the wild-type enzyme. For example, the single H257Y mutation relaxes the stereoselectivity for compounds **6**, **8**, and **11** from approximately 100:1 to less than 11:1. This single amino acid change can significantly diminish the enhanced stereoselectivity exhibited by G60A by up to 5 orders of magnitude (see, for example, compound **8**). Combinations of mutational changes can also be used to invert the stereoselectivity exhibited by the wild-type and G60A enzymes. The specific set of residues depends, in part, on the specific substituents attached to the central phosphorus core of the target substrate. Thus, the mutant H257Y/L303T is the best example for the inversion of compounds **5**, **6**, **14**, and **15**. With this set of compounds, the large substituent is either a phenyl or cyclohexyl group attached directly to the phosphorus core. A stereoselectivity as large as 1800 is observed for compound **14**. The mutant I106G/F132G/H257Y is the best enzyme for the inversion of stereoselectivity of compounds **7**, **8**, **11**, **12**, **13**,

(30) Hong, S.-B.; Raushel, F. M. *Biochemistry* **1996**, *35*, 10904−10912.

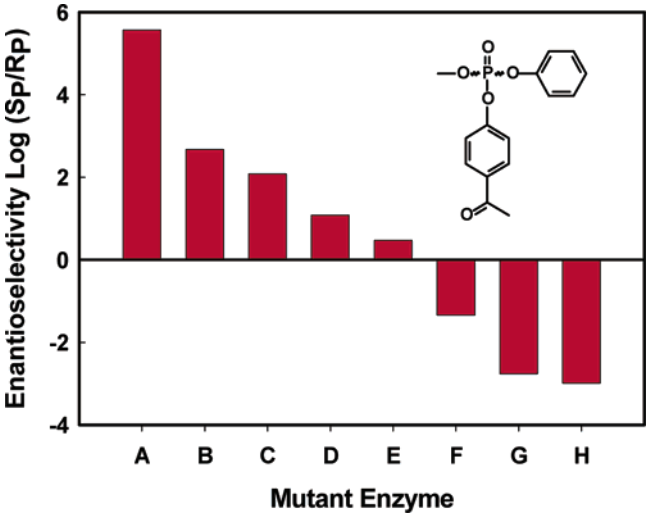

Figure 3. Enantioselectivity for the hydrolysis of compound **8** by the wild-type PTE and seven mutant enzymes at pH 9.0. The designated enzymes are as follows: A, G60A; B, S308G; C, wild-type PTE; D, I106G; E, I106G/F132G; F, I106T/F132A/H254G/H257W; G, I106G/H257Y; and H, I106G/F132G/H257Y.

and **16**. This collection of compounds invariably contains a phenolic or *O*-cyclohexyl group as the largest substituent attached to phosphorus. With these compounds, the stereoselectivity ranged from 12 to 970. The mutant I106A/F123A/H257W was the best enzyme for the inversion of stereoselectivity for compounds **1**, **2**, and **4**. With these compounds, the two substituents are relatively small, and the substituted amino acids have larger side chains in comparison to the mutant I106G/F132G/H257Y. Therefore, to a first approximation, the specific amino acids that are mutated in the active site of PTE can be selected and changed to a variety of residues that can be customized for a specified task.

The control of the enantioselectivity in this system is significant. For the wild-type enzyme, the stereoselectivity ranges from 1 to $>10^5$. For the single amino substitution, G60A, the stereoselectivity ranges from 6 to $>10^6$. As few as two to three amino acid changes within the active site of PTE can invert the inherent stereoselectivity such that the opposite enantiomer is the preferred substrate by a factor greater than 1000. Perhaps the most impressive range of stereoselectivity is exhibited for compound **8**. The mutant G60A prefers the S_P-enantiomer by a factor of 3.7×10^5, whereas the I106G/F132G/H257Y mutant prefers the R_P-enantiomer by a factor of 970. Therefore, the difference in stereoselectivity has been altered by a factor of 3.6×10^8 with only four amino acid changes! The range of enantioselectivity for compound **8** with the wild-type PTE and selected mutants is presented in Figure 3.

Structural Constraints on Stereoselectivity. What controls the inherent enantioselectivity of the wild-type enzyme and enables this catalytic property to be *relaxed*, *enhanced*, or *inverted* with relatively few amino acid changes within the active site? Some of the residues within the active site of PTE that coalesce to form the binding pockets for substrate recognition are presented in Figure 4.[19] Shown in this image is a non-hydrolyzed substrate analogue, diisopropyl methylphosphonate, which interacts through the phosphoryl oxygen to the β-metal ion in the active site. The overall binding pocket is largely hydrophobic, and there appears to be no strong electrostatic interactions between the protein and the substrate (other than

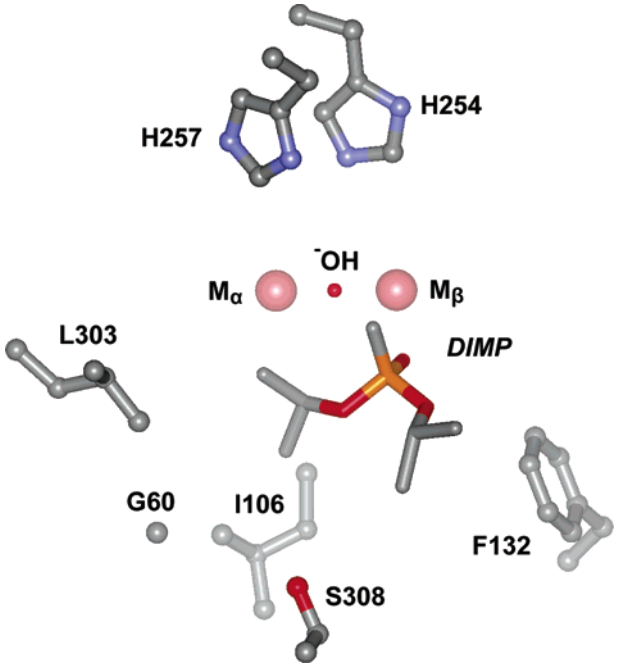

Figure 4. Structure of the active site of the wild-type PTE. The two divalent cations (M_α and M_β) are shown in salmon, and the bridging hydroxide is shown in red. The side chains and α-carbon atoms for the residues mutated in this investigation (G60, I106, F132, H254, H257, L303, and S308) are labeled. The substrate analogue, diisopropyl methylphosphonate (DIMP), is positioned adjacent to the binuclear metal center. The coordinates were taken from the PDB file 1ez2 and rendered with the program WebLab Viewer Pro.

Chart 2

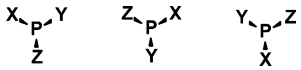

with the divalent cation). In this complex, there are subsites for each of the three substituents attached to the central phosphorus core.[19] In a productive enzyme−substrate complex, we assume that the leaving group must be positioned in a manner that will allow for a nucleophilic attack by the bridging hydroxide onto the substrate, with the leaving group orientated at an angle of approximately 180°.

Since the individual enantiomers have the same inherent chemical reactivity, the rate differential may be explained on the basis of differences in binding to the chiral active site. Either the binding is thermodynamically weak or the orientation of binding exhibited by the more poorly hydrolyzed enantiomer is unproductive. For the substrates examined in this analysis, there are three different substituents attached to the central phosphorus core. Each of the three substituents must be oriented in some manner within the active site. If one assumes that there are separate binding subsites for each of these substituents (X, Y, and Z), then there would be three possible orientations (or binding modes) for any given substrate. Since the leaving group must be aligned properly with the attacking nucleophile, only one of these three orientations will lead to productive turnover. These orientations are presented graphically in Chart 2. In this scenario, the slower enantiomer would have a preponderance of the bound substrate in one of the two possible nonproductive orientations. A more subtle distinction between the two enantiomers would position the slower enantiomer at a less optimal attack angle relative to the hydroxide nucleophile or bound to

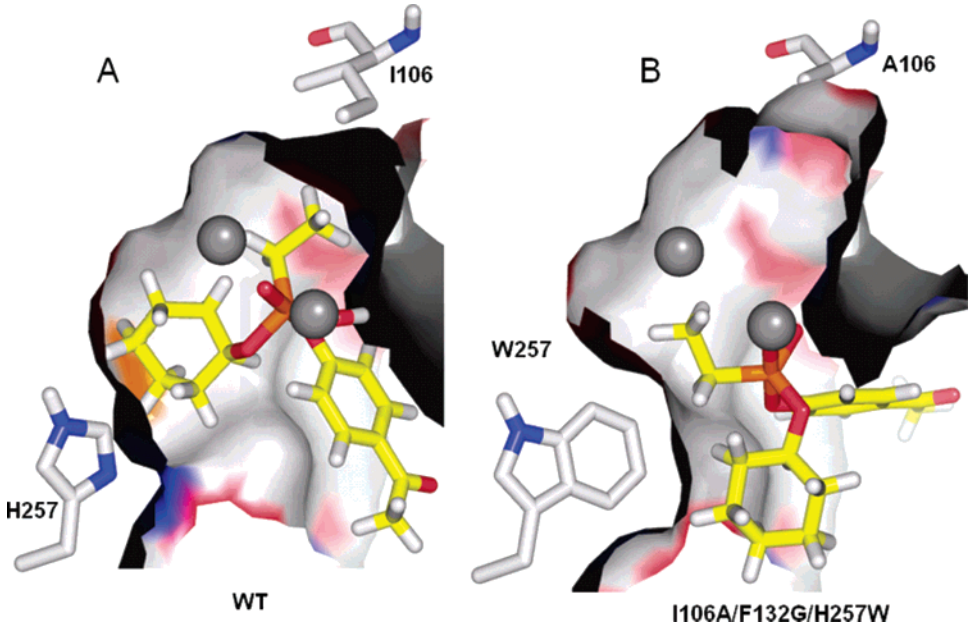

Figure 5. Changes in enantiomeric preference resulting from steric changes to key active-site residues for two docked structures of compound R$_P$-**13**, (A) WT PTE and (B) mutant I106A/F132G/H257W structures. In the WT structure, a catalytically competent geometry is found. This is less true in the mutant structure, presumably owing to the steric changes in site. Oxygen atoms are colored red, enzyme carbons in gray, ligand carbons in yellow, hydrogens in white, and nitrogens in blue. The molecular surface of the enzyme is shown, as are two of the residues whose sterics change the most on substitution. The gray spheres represent the two catalytic zinc ions. This figure was rendered using PyMOL.[32]

the active site such that the phosphoryl oxygen is unable to be polarized via a direct interaction with one of the two divalent cations. The acquisition of X-ray structures of PTE bound with chiral inhibitors will help to establish the root cause for the enantioselectivity of PTE and the site-directed mutants.

If simple sterics play a large role in selecting between productive and unproductive substrate geometries, as suggested by the preceding discussion, then it should be possible to capture by relatively simple calculations of molecular fit between substrate and enzyme. We turned to molecular docking calculations of high-energy intermediate forms of the substrates into model structures of 7 of the 15 mutant enzymes. The database of high-energy bipyramidal species of the substrates was docked into the active sites of the mutants, and for each pair of enantiomers the difference between their energy scores was calculated (see Supporting Information). This score is a proxy for the binding affinity, i.e., the stabilization of a compound by a PTE variant. The increase or decrease of the difference between docking energy scores for a pair of enantiomers in a mutant compared to the wild type (WT) should predict rate acceleration, deceleration, or even if the enantiomeric preference has been inverted between the WT and a given mutant enzyme.

In addition to the docking energy scores, we also considered the docked poses. We assumed that a catalytically competent pose (see Figure 5A) of an intermediate would place the former hydroxide between the two zinc ions, with the leaving group apical to that oxygen and oriented toward the exit of the active site in the leaving pocket. The two nonreactive side chains of the phosphorus core should be accommodated in the two subsites of the active site. A catalytically less competent pose (see Figure 5B) typically leaves one of the subsites empty (the small pocket in Figure 5B). As a secondary event to the less complementary steric fit, the resulting poses usually have impaired electrostatic interactions between the oxygens of the ligand and the zinc ions. The failure of DOCK,[31] the program used for docking, to find a catalytically optimal pose for a particular enantiomer suggests that a highly productive pose is unlikely to occur, making hydrolysis unlikely even when the energy score might be favorable.

Qualitatively, the enantiomeric selectivities predicted by docking correspond closely to the experimental results. Of the 29 experimentally observed inversions, 28 were predicted by docking either through a significant change of the energy difference between the two enantiomers or by the failure to find a catalytically correct pose for one of the two enantiomers (see Table 2 and Supporting Information for detailed docking scores). For five enantiomer−mutant pairs, an inversion was predicted that was not observed experimentally; four of these were for compound **6**. Similarly, the docking energies also qualitatively tracked those pairs in which the relative selectivities between the isomers changed from the WT, though the overall isomeric preference remained the same. For 13 of 20 mutant−enantiomer pairs, the docking scores can predict this acceleration and deceleration correctly. Here, too, 4 of the 7 wrong predictions owe to compound **6** alone. In all cases where DOCK failed to predict the change in the experimental ratio, this change was by a factor of about 10 or less compared to the WT. In those cases where the acceleration or deceleration was larger than 10-fold, this change of the ratios was captured correctly by the docking predictions.

An example of a dramatic change of the binding quality and energy due to a substitution is illustrated in Figure 5. The high-energy intermediate of compound R$_P$-**13** can be stabilized and bound well by the wild-type enzyme (Figure 5A), where the

(31) Meng, E. C.; Shoichet, B. K.; Kuntz, I. D. *J. Comput. Chem.* **1992**, *13*, 505−524.
(32) http://pymol.sourceforge.net/
(33) Hermann, J. C.; Ghanem, E.; Li, Y.; Raushel, F. M.; Irwin, J. J.; Soichet, B. K. *J. Am. Chem. Soc.* **2006**, *128*, http://dx.doi.org/10.1021/ja065860f.

Table 2. Stereoselectivities Predicted by Molecular Docking[a]

Compound	WT	G60A	I106G	H257Y L303T	I106G H257Y	I106G F132G H257Y	I106A F132A H257W	I106T F132A H254G H257W
1	R_P	↑		↻		↻	↻	↻
2	S_P	↑		↻			↻	↻
4	R_P	↑		↻		↻	↻	↻
5	S_P	↑	↑	↻		↑	↻	↻
6	S_P	↑	↑	↻	↑	↑		↑
7	R_P	↑	↓	↻		↻		↻
8	S_P	↑	↓		↻	↻		↻
11	R_P	↑	↓			↻		↻
12	S_P	↑				↻		
13	R_P	↑				↻	↻	↻
16	S_P	↑			↻	↻		

[a] Results are given relative to the ratio of rates of the wild type (see Table 1 and Supporting Information for more details). The wild-type preferences for an enantiomer are given in the "WT" column. In each case, the same enantiomer is favored by docking, as was experimentally verified. The arrows indicate the experimentally observed qualitative changes in enantioselectivity. The colors indicate whether docking was able to predict that change qualitatively. If an arrow is red, the docking prediction is incorrect; if it is black, docking predicted the experimental enantioselectivity correctly. Up arrows indicate an increase of the ratio of rates, down arrows indicate a decrease of the ratio of rates, and curving arrows indicate an inversion of the enantioselectivity.

oxygen is placed equidistant between the two zinc ions and all pockets are complemented by the side chains of the phosphorus core. Conversely, in the I106A/F132G/H257W mutant enzyme, no highly productive pose can be found for this compound (Figure 5B). The former small pocket—close to A106—is empty, and the oxygen is mainly interacting with one zinc ion only. For the enantiomer S_P-**13**, which has the two nonreactive side chains switched, the opposite can be observed: S_P-**13** fits well in the I106A/F132G/H257W mutant but not in the WT (not shown). Poses and energies suggest, for enantiomer pair **13**, that the R_P-enantiomer is preferred by the WT, whereas the S_P-enantiomer is preferred by the I106A/F132G/H257W mutant, which is consistent with the experimental results (see Table 1).

These results suggest that the changes in the ratio of rates and enantioselectivities of mutant PTEs are captured by relatively simple stereochemical and electrostatic effects. These effects can be represented by the geometry of the high-energy intermediates docked in these calculations. An important innovation in these calculations is docking not of ground-state substrate structure but rather of a high-energy intermediate that resembles a transition-state-like state (see accompanying paper for more discussion of this point).[33] As a caution, we note that docking, as used here, represents a relatively simple level of theory, and consequently this analysis cannot be pushed too far. Indeed, inspection of the docking energies shows that, whereas they qualitatively agree with the experimental changes in preferences, their quantitative agreement is poor (see Supporting Information). For instance, the ratio of rates for enantiomer pair 6 increases about 400-fold in the G60A mutant compared to the WT, which corresponds to a difference in docking scores of 0.5 kcal mol^{-1}. The ratio of rates for enantiomer **16** increases by a factor of 80 in the same mutant, which corresponds to an increase of 11.3 kcal mol^{-1} in the docking scores. So, even when docking predicts the correct direction of a ratio change very reliably, the magnitude of that change cannot be correlated with the difference in the docking scores for the two enantiomers.

Overall, these docking results support the hypothesis that the stereospecificity and efficiency of the PTE mutants can be directly related to the modification of the shape of the three hydrophobic binding pockets (the leaving group pocket and two subsites for the other side chains). Primarily, the mutations improve or disrupt the hydrophobic interactions between a compound and the enzyme. A secondary but nevertheless important distinguishing element is the polar interaction between the substrate oxygens and the catalytic zincs, which can change dramatically as a result of an unfavorable pose and orientation of a compound within the active site during catalysis.

Of course, to be compelling, it would be important to use these docking calculations prospectively, to predict enantioselectivities on previously untested substrates. We return to just such a study in the accompanying paper,[33] where the selectivities of several enantiomers on the part of the mutant enzymes were predicted before the results were known.

Summary. Wild-type and mutant forms of the bacterial phosphotriesterase have been shown to catalyze the stereoselective hydrolysis of racemic mixtures of chiral phosphate, phosphonate, and phosphinate esters. For the wild-type enzyme, one enantiomer can be preferred by up to 5 orders of magnitude. A single active-site mutant, G60A, enhances the inherent stereoselectivity of the wild-type enzyme by an additional 1−2 orders of magnitude. Mutations within the active site that expand and contract the size of the binding subsites can relax and invert the enantioselectivity of the wild-type PTE for the initially

slower enantiomer by up to 3 orders of magnitude. Molecular docking calculations suggest that the reason for these kinetic effects might be the impaired or improved stabilization of high-energy structures, owing to steric complementarity. This enantioselective enzyme library can be used to kinetically resolve chiral mixtures of racemic phosphorus-based esters.

Acknowledgment. This work was supported in part by the NIH (GM68550 and GM71790). J.C. and T.E. were supported by the NSF REU program CHE-0243829. J.C.H. thanks the "Deutschen Akademie der Naturforscher Leopoldina" for a fellowship under contract no. BMBF-LPD 9901/8-115.

Supporting Information Available: Detailed docking scores. This material is available free of charge via the Internet at http://pubs.acs.org.

JA0658618